COBEM 2023 27TH INTERNATIONAL CONGRESS OF MECHANICAL ENGENEERING

ABCM Brazilian Society of Mechanical Sciences and Engineering
27th ABCM International Congress of Mechanical Engineering
December 04-08, 2023, Florianópolis-SC, Brazil

COB-2023-0727
VERIFICATION BENCH BASED ON A CENTRIFUGAL FAN WITH VARIABLE SPEED FOR GAS FLOW METERS

Luciano Amaury dos Santos
Carlos Eduardo Orgecoski
Francisco Édson Nogueira de Melo
IFSC – Instituto Federal de Santa Catarina, Av. Mauro Ramos, 950 – Centro - CEP 88020-300 – Florianópolis - SC
luciano.santos@ifsc.edu.br, carlosorgecoski@gmail.com, edson.n.melo@gmail.com

João Paulo Cardoso Lacombe
SCGÁS – Companhia de Gás de Santa Catarina, Rua Antônio (Nico) Luz, 255 - Centro - CEP 88010-410 – Florianópolis - SC
joao.paulo.cardoso.lacombe@gmail.com

Abstract. *This work presents a bench, based on the use of a centrifugal fan commanded through a frequency inverter, for verifying gas flow meters. The gas meters usually have at least one "low frequency sensor", that at the end of the operational flow range switches below 1 Hz, and sometimes have also a "high frequency sensor" that switches above 1 kHz. This work also describes briefly a simple electronic circuit for detecting this switching and pieces of software needed to turn this switching in flow information, as well to gather pressure information and to change the fan speed when demanded. The most usual way of performing gas flow meter verifications is by the use of a reference meter mounted in series (traversed by the same air flow) with the meter to be verified. It was observed, however, that the response of a turbine type gas meter to the flow caused by a radial fan spinning at the same speed and blowing air in the same bench (a short pipe with the pressure sensor installed) is repetitive to a degree that allows the recording of the response of the reference gas meter and then its comparison to the response of other gas meters to be verified (at least if they are of the same model) dismissing the use of two gas meters in series. Further investigation also showed that a characteristic surface of the bench (the pressure head it supplies as a function of the air volumetric flow rate and the fan speed) could be used in this verification process (the characteristic surface obtained with a certain model of reference gas meter can be used to other models of gas meters to be verified, without putting them in series). The proposed bench has a relatively low cost (the most expensive component is the radial fan, and it is cheaper than a gas meter) and the discussion of its advantages and disadvantages, in light of the experimental results obtained and of what is known of other verification systems commercially available, is a valuable one.*

Keywords: *flow measurement, verification, natural gas, radial fan*

1. INTRODUCTION

The gas meters used by natural gas distribution companies to bill their customers are subject to periodic calibrations certified by accredited laboratories. To be calibrated the meters must be sent to one such very well equipped laboratory (Pandelova *et al.*, 2017) and, after a careful calibration, be sent back to the gas distributor. This is not an inexpensive nor quick process and accidents can happen while it evolves. The gas distributor will send a gas meter to calibration only if it is necessary and if the gas meter is in conditions of being calibrated. To ensure this it is essential to have a quick and inexpensive mean of verify if a gas meter is working reasonably in accordance to its specifications.

When the work developed by Orgecoski (2022) was started, technicians at SCGÁS were using small fans to create a weak air current, able to move the sensitive mechanisms of some gas meters, but not powerful enough to produce a flow that could be used in an effective verification of their measurements quality. The first step in the development of the verification equipment here described, was to search a blower able to cover the flow range of some of the gas meters used by SCGÁS allowing the identification of signs of degraded quality in their measurements. The bench was developed to check rotary lobe and turbine meters for flow rates up to 400 m³/h.

1.1 Alternative gas meters verification equipment

There are commercially available high quality mobile gas meter verification systems, such as those offered by Dresser Measurement (2023a). They are operated putting the meter to be verified in tandem with a reference meter incorporated into the system. Both meters are traversed by the air flow from an appropriate blower that, together with the instrumentation stays over a small trailer. The prices of such systems are usually not affordable to latin american gas distributors and

the maintenance of the reference meter traveling bumpy roads increases its operation costs.

Another verification method uses a piping arrangement called a meter prover (Automation Forum, 2023)(Emerson, 2023). These meter provers consists in piping sections that can be, through adequate valves manoeuvres, connected to and disconnected of the piping where the gas meter to be tested is installed. An sphere is injected into one of the prover extremities and, after the appropriate valves manoeuvre, it is pushed by the gas to the other. Measuring the time that the sphere takes to travel a path with known length and cross section area, the flow rate is easily calculated (and compared to the gas meter indication). This piping arrangement is expensive, permanently takes up considerable space in the client installation and has a time-consuming operation that involves extra safety precautions as it is performed using the natural gas itself at the typical working pressures of the installation.

So a gas meters verification system with lower costs of purchase and operation are very desirable in Latin America and possibly other less affluent parts of the world.

2. THE BENCH

Figure 1 shows the bench with a FMT-Lx $8''$ G250 (Flow Meter Group, 2023) turbine gas meter connected to it. At the left of the picture it is seen the centrifugal fan VCI-280 (IBRAM, 2023). Inside the electrical panel box standing in front of the fan is the frequency inverter CFW-10 (WEG, 2023a). Stuck in the 72 mm diameter pipe that runs from the fan discharge to the gas meter, 1 m to the right of the fan discharge mouth, is the pressure sensor MPS20N0040D (Hrisko, 2020). In front of the pressure sensor is a small plastic box containing an Arduino Nano and some additional electronics to receive the data from that sensor and of the gas meter and forward it to the portable computer in front of the gas meter. The computer also sends commands to the frequency inverter through that Arduino Nano (Arduino, 2023) with the help of a Darlington array (Texas Instruments, 2023) in this relaying.

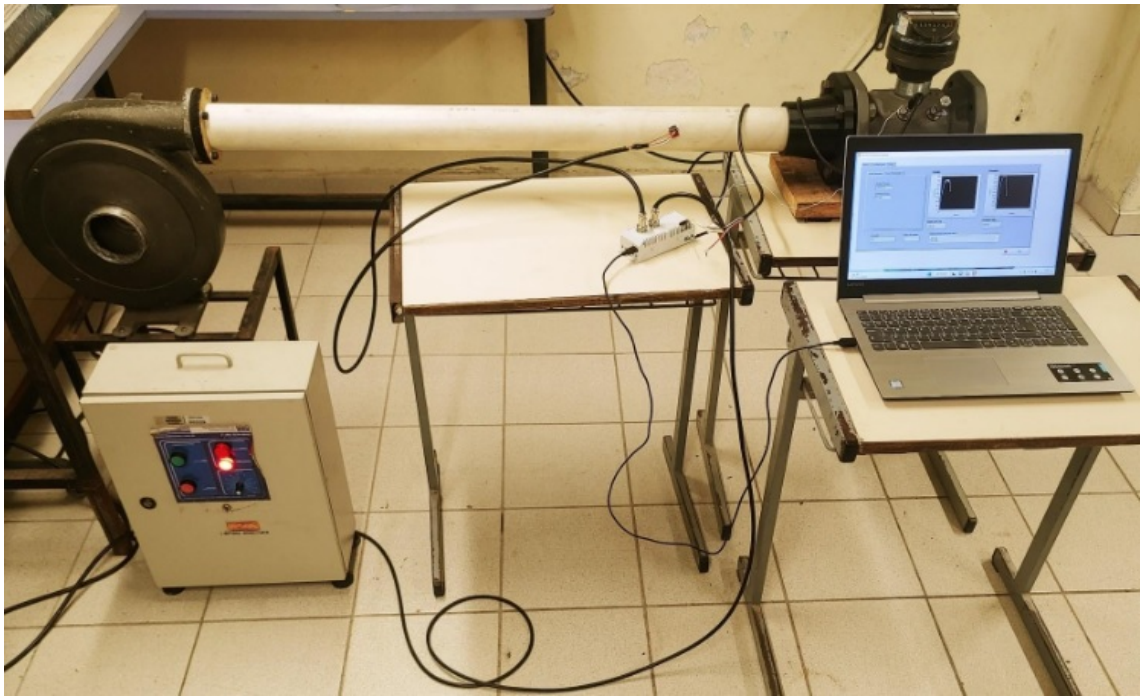

Figure 1. The verification bench testing a G250 turbine gas meter.

This apparatus allows gathering the values of three main variables: the selected fan rotational speed, the pressure due to the (small) gas meter resistance to the air passage throught it and the flow rate reading coming from the gas meter. The first goal the authors had in its use was to confirm that, if coarse perturbations near the inlet of the fan or the outlet of the gas meter are avoided, for a same fan rotational speed selected, the same pressure and flow readings would be obtained if the gas meter is not changed. In fact, less than 1 % of variation in such readings was observed with this FMT-Lx turbine gas meter at the most usual conditions. A few tests were made using a rotary lobe gas meter B3:8C175 G16 (Dresser Measurement, 2023b), but it was outworn and its response to the fan rotational speed did not had this repeatability, being quite sensitive to the lubrication of its mechanisms. It should be noted that this may not be a symptom of any problem that would affect flow rate measurement accuracy, in such a positive displacement gas meter, as it would be in a turbine gas meter. Some other relevant information about the bench will be given here, but a more detailed description is available in the work of Orgecoski (2022).

2.1 The electronic assembly

The electronic assembly that was developed to be incorporated at the bench here described is based on a Arduino Nano platform. The functions that this assembly must perform demanded the aggregation of other elements to the Nano. For this, enumerating the functions of the assembly is a convenient way of presenting these assembly parts.

1. The frequency inverter CFW-10 (WEG, 2023a) can be commanded remotely by switching connections between a 10 V borne and four digital inputs that it has, using what its manufacturer call MultiSpeed functionality. To control this switching (that allows start and stop the fan as well as to choose one of eight pre-programmed frequencies - rotational speeds) using four 5 V digital outputs of the Nano platform, a Darlington array (Texas Instruments, 2023) was added to the circuit (as mentioned previously).

2. Most of gas meters have at least one switch reed (or some solid state component with similar electrical behavior) low frequency sensor coupled to its mechanical totalizator mechanism. Turbine gas meters eventually also present a high frequency proximity sensor close to the turbine that works according to NAMUR standard (IEC 60947-5-6:1999) and so must be powered with 8.2 V. To provide the 8.2 V a DC-DC converter (Xi'an Aerosemi Technology, 2011) was connected to the regulated 5 V output of the Arduino Nano. It was observed that the signal connection of this high frequency sensor to one of the Nano platform digital inputs is the assembly part most susceptible to electromagnetic noise. So a careful grounding of this sensor and of the shielding of its cable is recommended.

3. The MPS20N0040D (Hrisko, 2020) pressure sensor has a four-wire digital output straightly connected to the Nano, not demanding any additional component besides cabling.

4. The Arduino Nano serial communication to a personal computer, through an USB cable is native, not demanding any additional component besides that USB cable.

2.2 The firmware

The Arduino Nano programming (that originates its firmware), using the Arduino IDE, was quite straightforward, just allowing the reception of the sensors readings and relaying the commands coming from the personal computer to the frequency inverter. It is interesting to note, however, that detecting the switching frequency coming form the gas meter sensor (that will be translated in a measure of the volumetric flow rate traversing it) may be challenging: the recommended approach when using the low frequency reed switch sensor installed at the gas meter totalizator is inadequate to the high frequency NAMUR sensor used near the turbine and vice-versa. This is because, to precisely detect the instant when the state of the digital input corresponding to a high frequency sensor changes, suspending all other types of interrupt to watch only that digital input (the `PulseIn()` Arduino function makes this very easy) is advisable, but obviously must be done at short regular time intervals, allowing the communication with other devices to happen most of the time. With a low frequency sensor this approach would make the Nano non-responsive for long times (in fact the typical pulse period of a gas meter low frequency sensor is longer than the default timeout of `PulseIn()`). So it is better, with low frequency sensors, do not suspend interrupts and accept a lower accuracy in the detected pulsation frequency.

2.3 The software

A quite complete software for operating this bench was developed using LabVIEW (NI, 2023). It allows the choice between an automatic test (where pre-selected fan rotational speeds are scanned, with corresponding measured flow rate and pressure stored when they reach a steady value at each speed) or a interactive test (where the operator chooses the fan rotational speeds while observing the measurements). More interestingly for what will be presented in the remaining of this paper, the software also offers the possibility of choosing between two different sources of reference flow rate values (to which those measured by the gas meter will be compared in the verification process). The most recommended option is to use stored flow rate values observed in former testing of a (reference) gas meter of certified good quality and of the same model of that being subject to verification. Eventually, however, these values from a reference gas meter (with the same aerodynamic behavior as the gas meter under verification) may not be available (for differences between gas meter models or if the gas meter presents changes in its response to the same fan rotational speed, as happened with the rotary lobe gas meter tested). In this situation the flow rate can be estimated using a model for its interrelation with the fan rotational speed and the pressure measurement, and this estimate can be used as reference, less reliable than values taken from a reference gas meter of the same model, but better than none.

3. MAIN VARIABLES INTERRELATION

The variables in question are: the fan rotational speed, the pressure caused by the gas meter resistance to the airflow through it, and the magnitude of the flow rate. What connects these three variable is the fluid dynamics and the most

complex part of it happens inside the centrifugal fan. For this reason some basic theory used to describe the behavior of this kind of turbomachine will be briefly reviewed. Two hypothesis are admitted throughout this work with no further discussion beyond this paragraph: (i) the flow is assumed to be incompressible, as no Mach number above 0.1 is expected, and (ii) the fan rotational speed is assumed to be proportional to the electrical current frequency imposed by the frequency inverter. This second hypothesis is reasonable, since frequency inverters are designed to minimize the slip from the synchrony between frequency and rotation speed. Fans, however, have their torque, to which the slip is essentially proportional (WEG, 2023b), crescent with rotational speed, therefore to use a tachometer to monitor this speed may be a good suggestion for a future work of this kind.

3.1 Fan characteristic curve and affinity laws

Although the use of frequency inverters is currently very widespread (and recommended, as it allows controlled variations of the flow driven by fans and pumps avoiding the energy waste and wear of parts associated with partially closed valves), the characteristic curves of pumps and centrifugal fans continue to be presented just as they were before these devices became affordable. This is not really a problem, since the principles of dimensional analysis and similarity, presented e.g. in the Chapter 7 of Fox *et al.* (2022), can be used. In the case of pumps, fans and other turbomachines that typically work without appreciable compressibility effects), two dimensionless parameters (which remain the same in similar machines operating at analogous operating points) appear unequivocally (Lewis, 1996). The first one is the flow coefficient

$$\Phi = \frac{Q}{ND^3} \tag{1}$$

where Q is the flow rate (given in m³/s in SI), N is the rotational frequency (in Hz) and D is the diameter of the machine rotor (in m). The second is the head coefficient

$$\Psi = \frac{\Delta p}{\rho\,(ND)^2} \tag{2}$$

where Δp is the pressure difference (in Pa) between the discharge and suction of the machine, ρ is the specific mass of the air (in kg/m³) and the other variables have already appeared in the definition of the flow coefficient. In addition to these parameters, other parameters are eventually defined, such as the power coefficient and the specific velocity, which can be obtained as a combination of those presented here (but are not used in the present work).

If, not only compressibility, but also viscosity effects could be disregarded, these two parameter would have a functional relation that is the dimensionless characteristic curve of the machine shape. For only a nominal value of rotational speed and a chosen rotor diameter, the characteristic curve is usually given by the manufacturer as a relation between pressure difference (or, dividing this difference by the working fluid specific weight, head) and volumetric flow rate. For predicting the behavior of a fan or pump at any rotational speed (and the behaviour of a machine **with the same shape**, but with a different size), from the curve $\Psi = \Psi(\Phi)$ that can be obtained testing a single machine operating at a single rotational one have to rely on the Affinity laws (2023) or similarity (Fernandes Filho, 2015).

Figure 2 shows a dimensionless version of the characteristic curve given by the manufacturer of the fan IBRAM (2023) used in the bench and most of the measurement points obtained along the present work. The experimental points lie far from the characteristic curve by distances larger than the uncertainties of the measurements. This is not hard to explain as the measurement of pressure difference in the experiments here reported and in the determination of the characteristic curve (ANSI/AMCA 210-16 / ASHRAE 51-16) were not performed exactly in the same way. But a more dreadful feature is visible in Fig. 2, the experimental points cannot be described by any single curve. This means that they do not follow the affinity laws mentioned in the preceding paragraph.

The clue to understand this conflict between practice and simplified theory lies in the absence of the viscosity in Eqs. (1) and (2). The experimental points were obtained at very different rotational speeds, many becoming much more distant of the fan optimal operation point than it is usual. In such conditions not only impeller blades stall eventually happens, but also less dramatic viscous effects become important. So a third dimensionless parameter must be introduced and it is usually the machine Reynolds number

$$Re = \frac{\rho\, N\, D^2}{\mu} \tag{3}$$

where μ is the air kinematic viscosity (measured in Pa·s). Now, with three parameters, one has to deal with a characteristic surface instead of a characteristic curve.

3.2 The bench characteristic surface

The curve shown in Fig. 2 is just a third degree polynomial. No single surface equation reasonably simple, however, seemed to represent the experimental data gathered in the present work. The best alternative found by the authors was the

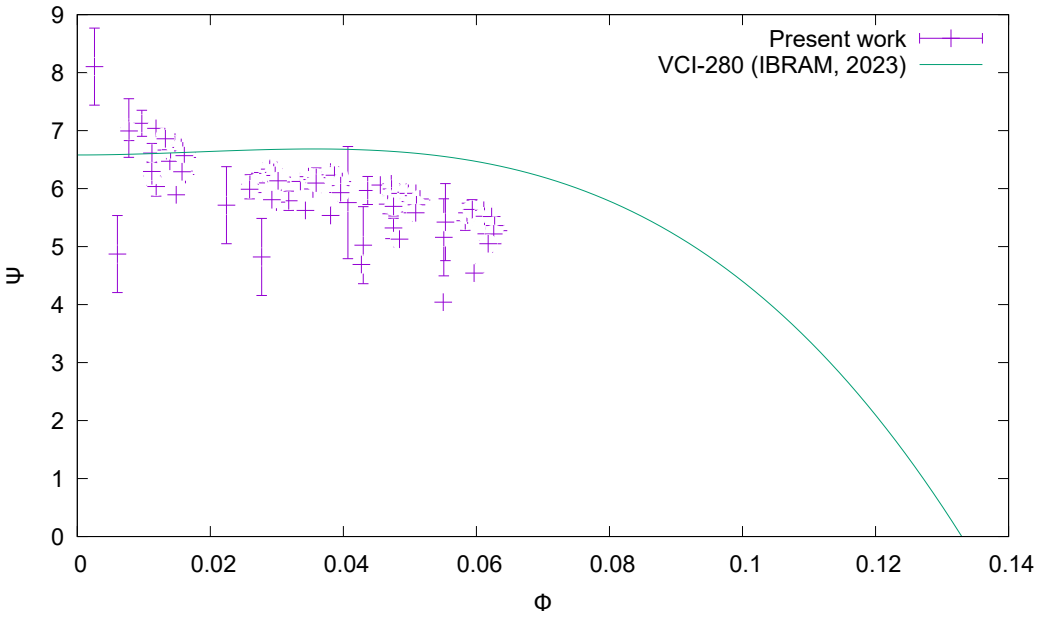

Figure 2. Fan characteristic curve and experimental data points collected in the present work.

use of the following pair of third degree two-dimensional polynomials

$$\Psi_{\mathrm{H}}(Re,\Phi) = \sum_{j=0}^{3}\sum_{i=0}^{3-j} a_{ij}\,(Re-c)^i\Phi^j \qquad \text{for} \qquad Re \geq c \tag{4}$$

$$\Psi_{\mathrm{L}}(Re,\Phi) = \sum_{j=0}^{3}\sum_{i=0}^{3-j} b_{ij}\,(Re-c)^i\Phi^j \qquad \text{for} \qquad Re \leq c \tag{5}$$

obeying the matching conditions

$$\Psi_{\mathrm{H}}(c,\Phi) = \Psi_{\mathrm{L}}(c,\Phi) \qquad \Longrightarrow \qquad a_{0j} = b_{0j} \qquad \text{for} \quad j = 0,1,2,3 \tag{6}$$

$$\left.\frac{\partial\Psi_{\mathrm{H}}}{\partial Re}\right|_{Re=c} = \left.\frac{\partial\Psi_{\mathrm{L}}}{\partial Re}\right|_{Re=c} \qquad \Longrightarrow \qquad a_{1j} = b_{1j} \qquad \text{for} \quad j = 0,1,2 \tag{7}$$

in such a way that

$$\Psi\,(Re,\Phi) = \begin{cases} \Psi_{\mathrm{H}}(Re,\Phi) & \text{if} \quad Re \geq c \\ \\ \Psi_{\mathrm{L}}(Re,\Phi) & \text{if} \quad Re < c \end{cases} \tag{8}$$

becomes a kind of spline surface. The coefficients a_{ij} and a_{ij} for i and j running from 0 to 3 and the seam position c were obtained using the nonlinear weighted least squares algorithm implemented in gnuplot (Williams *et al.*, 2022) with weighting based on the uncertainties estimates represented by the error bars in Fig. 2. The numbers presented in Tab. 1 may help in figuring out that Eqs. (4) to (8) are more practical than they look. The resulting surface is represented by the grid with contours in Fig. 3, the experimental data points scattered over it.

The beauty of Eq. (8) is that it allows the calculation of the flow rate, given the rotational speed of the fan and the pressure difference measured at the bench. A nonlinear equation must be solved in this process, but it is a third degree polynomial, although being more usual to the use iterative solutions, even exact formulas are available for solving it. A sequence of steps to perform this calculations is shown below:

1. with the rotational speed, the rotor diameter and air properties, the Reynolds number *Re* is given by Eq. (3);
2. with the measured pressure, the same speed and diameter, the head coefficient Ψ is given by Eq. (2);
3. with Re and Ψ known, the determination of the flow coefficient Φ is essentially the search for a real root of a third degree polynomial given by Eq. (4) or Eq. (5), depending on how Re compares to c;

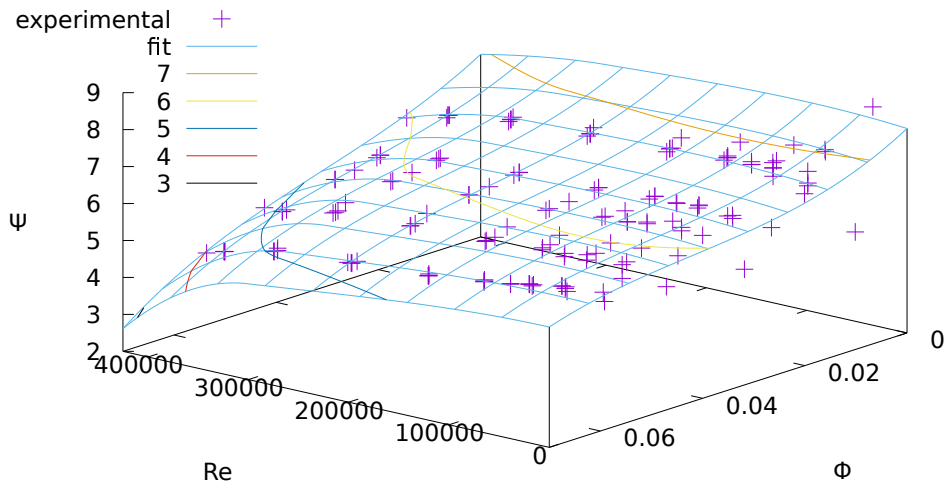

Figure 3. The surface (cyan grid with coloured contours at levels $\Psi = 3, 4, 5, 6, 7$) fitted to the experimental data points (violet crosses).

Table 1. Coefficients and seam position obtained fitting Eq. 8 to experimental data with Gnuplot (Williams *et al.*, 2022).

$a_{00} = b_{00} = 7.42446$ $a_{10} = b_{10} = -1.57281\times10^{-6}$ $a_{20} = -2.27792\times10^{-11}$ $a_{30} = 3.46201\times10^{-17}$	$a_{01} = b_{01} = -71.4924$ $a_{11} = b_{11} = 5.36384\times10^{-5}$ $a_{21} = -1.22334\times10^{-9}$	$a_{02} = b_{02} = 1399.11$ $a_{12} = b_{12} = -0.00104604$	$a_{03} = b_{03} = -13664.7$
$b_{20} = 8.69483\times10^{-13}$ $b_{30} = 1.63171\times10^{-17}$	$b_{21} = 2.3021\times10^{-11}$		
$c = 300623$			

4. with Φ found, the flow rate is determined inverting Eq. (1) to get

$$Q = ND^3\Phi \tag{9}$$

These steps were implemented using LabVIEW in the software mentioned in subsection 2.3.

3.3 Discussion and possible improvement paths

The deviations between the data-points and the fitted surface are around 15 %, being even higher at very low Reynolds numbers and very low flow coefficients. Such high errors seem to be due to an inadequacy of the MPS20N0040D (Hrisko, 2020) pressure sensor. Its range is nominally 40 kPa (but this should be taken with a grain of salt, as the information in the data sheet is not quite reliable) much larger than what is really needed for the kind of tests performed: the pressures measured in the present work barely reached 3 kPa. A better choice of pressure sensor, e.g., the use of a SM6331-BCE-S-004.00-431 (TE Connectivity, 2023), could have largely improved the accuracy of this model of the bench aerodynamic behavior.

Even with good pressure sensors, the pressure produced by a low velocity airflow is usually very low and then hard to measure. If this was the only problem the solution could be to use, simultaneously with a normal range pressure sensor, a low range but tolerant to high pressure sensor like SDP810-125Pa (Sensirion, 2022). But there is also a problem associated to the almost horizontal appearance of part of the characteristic curve in Fig. 2 observable also in sections of the surface in Fig. 3, and is mathematically expressed as

$$\frac{\partial\Psi}{\partial\Phi} \approx 0 \qquad \Longrightarrow \qquad \frac{\partial\Phi}{\partial\Psi} \approx \infty \tag{10}$$

This last approximation means that small errors in measuring the head coefficient will lead, in those regions of the model domain, to large errors in the calculation of the flow coefficient. Reviewing the standard uncertainty propagation models

(JCGM 100:2008) can make this clearer. For this reason the use of a low cost highly reliable hot film air mass flow sensor (Bosch I-Business, 2023) as a reference flow rate sensor in tandem with the sensor being verified will be (at least sometimes) safer than using the model here discussed.

A different way of dealing with the difficulties found in positive displacement gas meters verification is not so low cost: to use a twin lobe blower (Omel, 2023; Howden, 2023) instead of the centrifugal fan. As the twin lobe blower itself is a positive displacement blower, the relation between the flow rate and the (twin lobe) rotational speed would be almost independent of the restriction to the air flow caused by the gas meter. In such context the uncertainty amplification associated with Eq. 10 and another related question, that is the flow instability at small flow rates (to which centrifugal fans may be susceptible), simply do not occur.

3.4 Plant characteristic curves of the gas meters and additional remarks

The straight pipe until the pressure tap may be considered an extension of the fan and what was called here the bench characteristic surface describes the behavior of this extended fan. The gas meter, together with the pipe length downstream from the pressure tap and with the fitting used to connect this pipe to the gas meter, may be considered a ductwork (plant) imposing a pressure head to that extended fan. The plant characteristic curve (in terms of head and flow rate) is generally presented together with the pump or fan characteristic curve (in terms of the same variables) to show their intersection as the operation point of the system, e.g. Fig. 6.1 in Fernandes Filho (2015) or Fig. 10.17 in Fox *et al.* (2022). It is interesting to note that the plant characteristic corresponding to the gas meter and its fitting to the pipe coming from the fan may be obtained using the flow rate given by the gas meter itself (if it is well calibrated) and the same pressure sensor used to obtain the extended fan characteristic surface. This is not obvious but in fact this plant characteristic surface may be obtained using a subset (corresponding to that particular gas meter with its outlet unobstructed) of the data used for building the surface shown in Fig. 3. What makes this a little awkward is that, in describing the gas meter behavior, references to the fan rotational speed do not make sense: the gas meter receives a flow rate and responds to it with a pressure head (or vice-versa), so if dimensionless variables are to be used, they can not be those defined in Eqs. (1) to (3). For this reason, to produce the following Figs. 4 and 5, were used the minor head loss coefficient

$$K_{\text{l}} = \frac{\pi\,\Delta P\,D_{\text{p}}^4}{8\,\rho\,Q^2} \tag{11}$$

and the pipe Reynolds number

$$Re_{\text{p}} = \frac{4\,\rho\,Q}{\pi\mu D_{\text{p}}} \tag{12}$$

where D_{p} is the pipe diameter, the remaining variables already appeared in Eqs. (1) to (3).

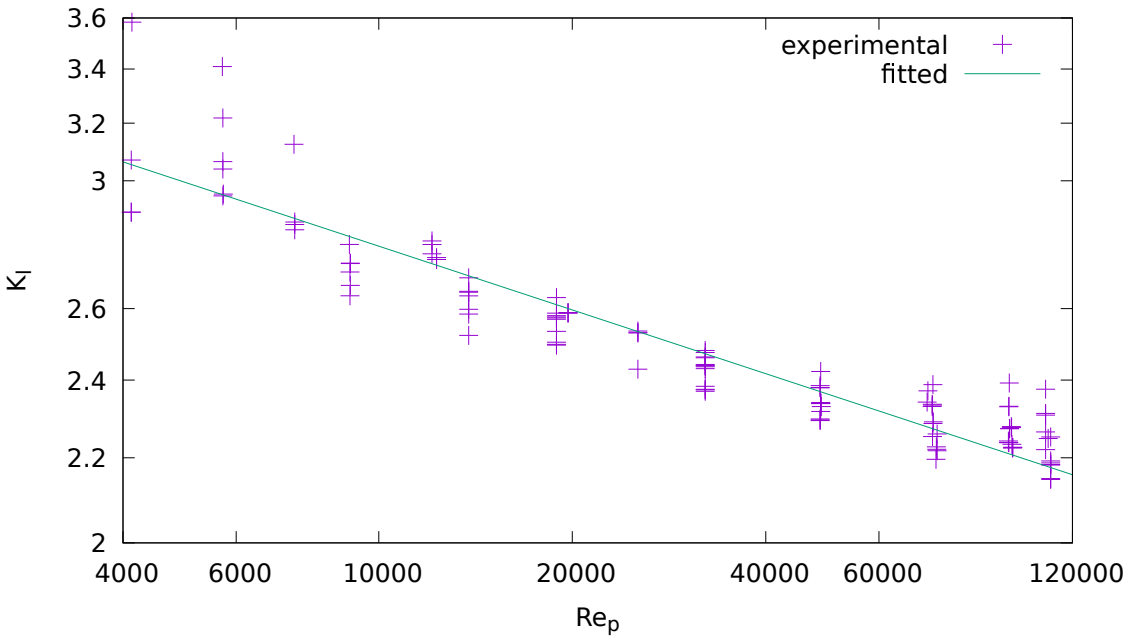

Figure 4. Plant characteristic for turbine gas meter LMT-Lx G250, experimental points and fitted curve $K_{\text{l}} = 7.2\,Re_{\text{p}}^{-0.103}$.

It can be seen in Fig. 4 that the pipe Reynolds number and the minor loss coefficients in these tests were really typical of most common problems in piping engineering. The arrange of the experimental values in groups of points vertically aligned is associated to the use of a same series of fan rotational speeds, repeatedly, **always being obtained the same flow rate for each rotational speed of the series** at each repetition. The dispersion of the loss coefficients also calls attention. To make a coarse measure of this dispersion it can be taken the deviation from the median, (half the difference between the larger and the smaller value corresponding to any given Reynolds number - **this is essentially what was used to estimate uncertainties when they were needed in the present work**) and it is found a value of almost 11 % of the median.

The number after the letter G in the gas meter model designation at the figure labels indicates the gas meter maximum operation flow rate, in cubic feet per minute.

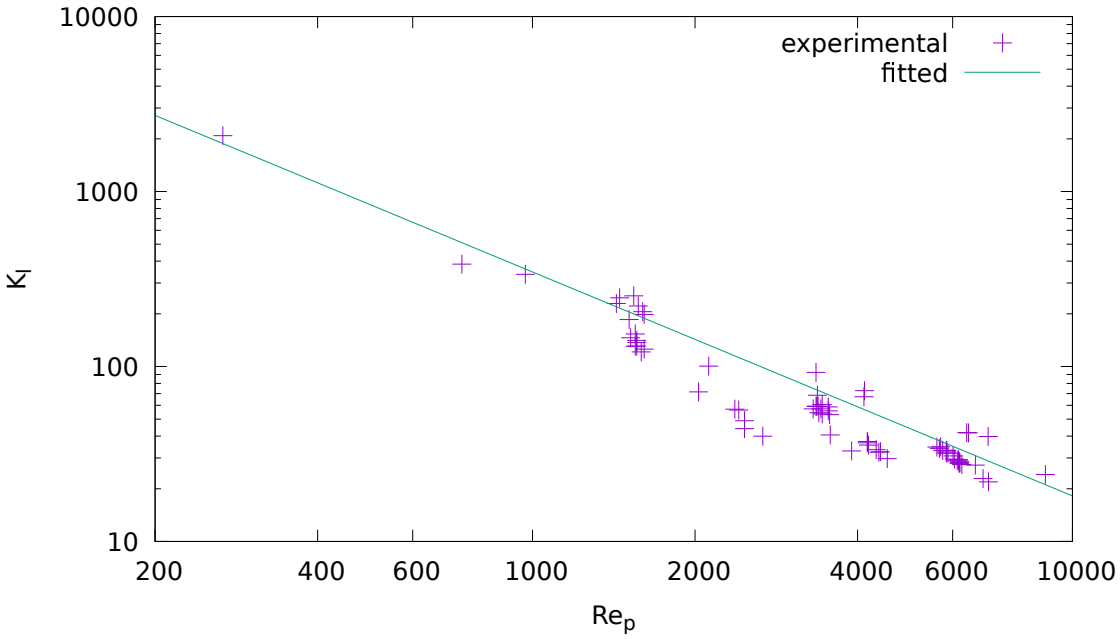

Figure 5. Plant characteristic curve associated to the rotary lobes gas meter B3:8C175 G16, experimental points and fitted curve $K_l = 2.4 \times 10^6 \, Re_p^{-1.28}$.

At first glace it may appear that the dispersion of the experimental data in Fig. 5 is smaller than that in Fig. 4, but if attention is paid to the vertical scale, immediately becomes clear that the minor losses coefficient values in Fig. 5 are orders of magnitude greater than those in Fig. 4. Using the same deviation from median measure of dispersion discussed at the preceding paragraph, the maximum value found is around 46 %. A large part of this dispersion may be attributed to the deficiency of the pressure sensor. The fact that the experimental results in this graph are not distributed in groups of points vertically aligned, however, highlights the fact that the flow rates (measured with the positive displacement B3:8C175 G16 meter) drifted significantly, between tests where the same rotational speed was imposed to the fan.

The dispersion shown in these graphs can make some readers intrigued about the possibility of eliminating it using averaging. To some degree this really can be made **averaging the results of multiple experiments**. The use of moving averages (or some other kind of low-pass digital filter) along each experiment, however, is rather ineffective in the present case. Averages of small series of values returned by subsequent calls (at 100 ms intervals) to the routine in use (Russell, 2015) to read the pressure sensor digital signal were performed and no reduction of the experiments results dispersion was perceived. The great difficulty is that the main source of dispersion is not any ergodic stochastic process, but a kind of hysteresis: if the sensor is pressurized from the atmospheric pressure to some kPa above it, after returning to the atmospheric pressure its output does not get back to its initial level (differing from it by an amount apparently unpredictable, but with modulus no greater than that corresponding to 16 Pa, in the tests conducted by the authors). Maybe this detail, observable when calibrating the sensor, is the only one really lacking in the very good presentation of the MPS20N0040D made by Hrisko (2020).

4. CONCLUSION

A gas meters verification bench, less expensive than those currently commercially available, but not as cheap as a small fan used to impose just some movement to the gas meter mechanisms, was developed. It worked quite well in the tests

performed, but it is larger and costs a little more than it was intended in the beginning of the project. Some improvement and adaptation to specific needs certainly can be made using the experience gathered and ideas developed in the prototype here described.

Testing the turbine gas meter, pretty small deviations, lower than 2 %, were obtained using a data base of reference flow rate values (from previous tests with a reference gas meters of the same model). Larger deviations (around 15 %) were found using a model for the bench behaviour (interrelation between the flow rate, the fan rotational speed and the pressure due to the resistance of the gas meter to the airflow through it) obtained fitting a spline surface to a large number of experimental data points. This is probably due to an inadequacy of the pressure sensor used in the present work (that brought inaccuracy to the data used to fit the surface and also to that used to test the model). But this model was not even part of the plans when this work begun (this was the reason for the use of a not very well suited pressure sensor that, however, was readily available) and it is more an interesting byproduct than a disappointing result.

Finishing the present work its authors reached the conclusion that, for some (positive displacement) gas meters, the use of a data base of flow rates corresponding to different fan rotational speeds and gas meters would not be accurate. They realized also that, in some regions of the bench characteristic surface, where the head coefficient is insensitive to moderate variations in flow coefficient, even measuring pressure with reasonable accuracy would not allow an accurate flow rate estimate. Only then they were able to appreciate Prof. E.W. Teichmann's suggestion of using an air mass flow (MAF) sensor (of the kind present in almost every ICE vehicle manufactured nowadays) as a reference flow rate sensor assembled in tandem with the gas meter to be verified. To adapt the bench here described to incorporate this sensor would demand a second DC-DC converter (supplying 12 V to power the sensor) and the substitution of the fan for another slightly more powerful, if the same flow rates range is to be covered (as the total head loss in the air circuit will be increased by this additional component). Checking how effective, accurate and reliable this will be is left to future works.

5. ACKNOWLEDGEMENTS

The authors acknowledge the support of SCGÁS and IFSC to this work. They are also thankful to Prof. E.W. Teichmann (DAMM - IFSC), for his suggestions and constant incentive, to Prof. F.R.M. da Mota, for donating the pressure sensor, to Prof. H.C. Pavanati (DAMM - IFSC), for providing the laboratory floor, to Prof. M.H. Mantelli (LEPTEN/LABTUCAL - UFSC), for lending the centrifugal fan and the frequency inverter used in the prototype and the water column manometer used in the pressure sensor calibration, and to Tech. C.N. da Silva (DAMM - IFSC and LEPTEN/LABTUCAL - UFSC), for the help in finding and lending this crucial equipment. Their gratitude is also deserved by many other colleagues and students at IFSC, specially those of the Technical Course in Mechanics and those working in the IFMaker for the help in designing and manufacturing prototype pieces.

6. REFERENCES

Affinity laws, 2023. "Wikipedia". Wikimedia Foundation. URL https://en.wikipedia.org/wiki/Affinity_laws.

ANSI/AMCA 210-16 / ASHRAE 51-16, 2016. "Laboratory methods of testing fans for certified aerodynamic performance rating". Standard, Air Movement and Control Association International, Inc. URL https://www.amca.org/assets/resources/public/pdf/Education%20Modules/AMCA%20210-16.pdf.

Arduino, 2023. "What is Arduino?" URL https://www.ni.com/pt-br/shop/labview.html.

Automation Forum, 2023. "What is a meter prover?" URL https://automationforum.co/what-is-a-meter-prover/.

Bosch I-Business, 2023. "Sensors for industrial and off-highway applications". Robert Bosch GmbH. URL https://www.bosch-ibusiness.com/media/images/products/sensors/xx_pdfs_1/sensors_catalog_01-2023.pdf.

Dresser Measurement, 2023a. "Accuracy testing". Dresser Utility Solutions. URL https://dresserutility.com/dresser-measurement/asset-management/ease-of-maintenance/accuracy-testing/.

Dresser Measurement, 2023b. "Rotary meters". Dresser Utility Solutions. URL https://dresserutility.com/dresser-measurement/rotary-meters-2/.

Emerson, 2023. "Meter provers". Emerson Electric Co. URL https://www.emerson.com/en-br/automation/measurement-instrumentation/flow-measurement/about-prover-systems.

Fernandes Filho, G.E.F., 2015. *Pumps, fans and compressors - funtamentals (in Portuguese)*. Saraiva. URL https://app.minhabiblioteca.com.br/reader/books/9788536519630/pageid/170.

Flow Meter Group, 2023. "FMT-Lx". Flow Meter Group B.V. URL https://www.flowmetergroup.com/product/fmt-lx/.

Fox, R.W., McDonald, A.T. and Mitchell, J.W., 2022. *Fox and McDonald's introduction to fluid mechanics*. John Wiley Sons, New York, 10th edition.

Howden, 2023. "Roots PD blowers". Howden Group. URL https://www.howden.com/en-gb/products/blowers/roots-lobe-blowers/roots-pd-b

lowers.

Hrisko, J., 2020. "MPS20N0040D pressure sensor calibration with Arduino". Maker Portal. URL https://makersportal.com/blog/2020/6/4/mps20n0040d-pressure-sensor-calibration-with-arduino.

IBRAM, 2023. "Centrifugal fan VCI (in portuguese)". Indústria Brasileira de Máquinas Ltda. URL https://www.ibram.ind.br/ventilador_centrifugo_vci.php.

IEC 60947-5-6:1999, 1999. "Low-voltage switchgear and controlgear - part 5-6: Control circuit devices and switching elements - DC interface for proximity sensors and switching amplifiers (NAMUR)". Standard, International Electrotechnical Commission. URL https://webstore.iec.ch/publication/3995.

JCGM 100:2008, 2008. "Evaluation of measurement data – guide to the expression of uncertainty in measurement". Standard, Joint Committee for Guides in Metrology. URL https://www.bipm.org/documents/20126/2071204/JCGM_100_2008_E.pdff.

Lewis, R.I., 1996. *Turbomachinery performance analysis*. Elsevier.

NI, 2023. "What is LabVIEW?" National Instruments Corp. URL https://www.ni.com/pt-br/shop/labview.html.

Omel, 2023. "Roots blowers". OMEL Bombas e Compressores Ltda. URL https://www.omel.com.br/en/our-products/roots-blowers/.

Orgecoski, C.E., 2022. "Gas meters verification system (in Portuguese)". Mechatronics Engineering course completion work, Instituto Federal de Santa Catarina.

Pandelova, A., Aleksandrova, T. and Chavdarova, Z., 2017. "Calibration of gas flow meter with test bench ITF2500-1-A". *Metrology and Metrology Assurance*, pp. 101–106. URL https://metrology-bg.org/fulltextpapers/339.pdf.

Russell, S., 2015. "Queuetue HX711 Arduino library". Available in the Arduino IDE Library Manager and at GitHub. URL https://github.com/queuetue/Q2-HX711-Arduino-Library.

Sensirion, 2022. "SDP810-125Pa: digital DP sensor (±125 Pa), tube connection". Sensirion AG. URL https://sensirion.com/products/catalog/SDP810-125Pa.

TE Connectivity, 2023. "SM6331-BCE-S-004.00-431 – 4 kPa diff. digital pressure sensor". URL https://www.te.com/usa-en/product-6331-BCE-S-004-000.html.

Texas Instruments, 2023. "ULN2803C – 50 V, eight-channel darlington array". Texas Instruments Inc. URL https://www.ti.com/product/ULN2803C.

WEG, 2023a. "Frequency inverter – CFW10 series". WEG S.A. URL https://www.weg.net/catalog/weg/NI/en/Drives/Legacy-Drives/Variable-Speed-Drive-CFW10/Frequency-Inverter---CFW10-Series/p/MKT_WDC_GLOBAL_FREQUENCY_INVERTER_EASY_DRIVE_CFW10.

WEG, 2023b. "Specification guide – electric motors". WEG S.A. URL https://static2.weg.net/medias/downloadcenter/ha0/h5f/WEG-motors-specification-of-electric-motors-50039409-brochure-english-web.pdf.

Williams, T., Kelley, C. and many others, 2022. "gnuplot 5.4 – an interactive plotting program". gnuplot homepage. URL http://www.gnuplot.info/.

Xi'an Aerosemi Technology, 2011. "MT3608: 2 A, high efficiency, 1.2 MHz step-up converter". DatasheetsPDF. URL https://datasheetspdf.com/pdf/909246/AEROSEMI/MT3608/1.

7. RESPONSIBILITY NOTICE

The authors are solely responsible for the printed material included in this paper.